An Electron-Deficient Triosmium Cluster Containing the Thianthrene Ligand: Synthesis, Structure and Reactivity of $[Os_3(CO)_9(\mu_3\text{-}\eta^2\text{-}C_{12}H_7S_2)(\mu\text{-}H)]$

Arun K. Raha,[1] Mohammad R. Hassan,[1] Shariff E. Kabir, *,[1] Md. Manzurul Karim,[1] Brian K. Nicholson, *,[2] Ayesha Sharmin,[3] Luca Salassa[3] Edward Rosenberg,*,[3]

[1]Department of Chemistry, Jahangirnagar University, Savar, Dhaka 1342, Bangladesh

[2]Department of Chemistry, University of Waikato, Hamilton, New Zealand

[3]Department of Chemistry, The University of Montana, Missoula, Montana 59812, USA

ABSTRACT

Reaction of $[Os_3(CO)_{10}(CH_3CN)_2]$ with thianthrene at 80 ^oC leads to the nonacarbonyl dihydride compound $[Os_3(CO)_9(\mu\text{-}3,4\text{-}\eta^2\text{-}C_{12}H_6S_2)(\mu\text{-}H)_2]$ (**1**) and the 46-electron monohydride compound $[Os_3(CO)_9(\mu_3\text{-}\eta^2\text{-}C_{12}H_7S_2)(\mu\text{-}H)]$ (**2**). Compound **2** reacts reversibly with CO to give the CO adduct $[Os_3(CO)_{10}(\mu\text{-}\eta^2\text{-}C_{12}H_7S_2)(\mu\text{-}H)]$ (**3**) whereas with PPh_3 it gives the addition product $[Os_3(CO)_9)(PPh_3)(\mu\text{-}\eta^2\text{-}C_{12}H_7S_2)(\mu\text{-}H)]$ (**4**) as well as the substitution product 1,2-$[Os_3(CO)_{10}((PPh_3)_2]$ (**5**). Compound **2** represents a unique example of an electron-deficient triosmium cluster in which the thianthrene ring is bound to cluster by coordination of the sulfur lone pair and a three-center-two-electron bond with the C(2) carbon which bridges the same edge of the triangle as the hydride. Electrochemical and DFT studies which elucidate the electronic properties of **2** are reported.

KEY WORDS: Triosmium cluster; Thianthrene; Electron-deficient; Ligand addition; DFT

INTRODUCTION

The synthesis and reactivity of electron-deficient benzoheterocyclic triosmium clusters, $[Os_3(CO)_9\{\mu_3\text{-}\eta^2\text{-}(L\text{-}H)\}(\mu\text{-}H)]$, (L = quinolines, phenanthridine, 5,6-benzoquinoline) where the electron-deficiency arises from the presence of a three-center two-electron bond β to the coordinated pyridinyl nitrogen, have been studied intensively over the last ten years because of their unique structures, fascinating chemical reactivity and particularly their applications in modelling industrially important catalytic processes [1-7]. Even in cases of heterocycles containing two heteroatoms such as a second nitrogen, sulfur or oxygen and as well as nitrogen and a fused benzene ring (e.g., quinoxaline, benzimidazoles, benzothiazoles, benzoxazoles) the products are the results of C-H activation at C(7) (C(8) for quinoxaline) and nitrogen coordination. These decacarbonyl complexes cleanly decarbonylate to give structural analogs of the complexes obtained with the nitrogen containing benzoheterocycles, $[Os_3(CO)_9\{\mu_3\text{-}\eta^2\text{-}(L\text{-}H)\}(\mu\text{-}H)]$, (L = benzimidazoles, benzothiazoles, benzoxazoles, qunoxaline) [2,3] An interesting feature of all of these electron-deficient clusters is that reactions with nucleophiles such as phosphines and amines result in ligand addition at the metal core [1a, b] while with anionic nucleophiles such as hydride or carbanions nucleophilic addition is at the carbocyclic ring [1c, 3]. The latter represents a dramatic change of the reactivity of the coordinated heterocyclic ligands relative to the free ligand where reaction with anionic nucleophiles is always at the heterocyclic ring. We have also demonstrated that despite their structural similarities, the reactivity of these compounds is sensitive to the nature of the heterocyclic ring [2-5]. In the case of the heterocycles containing two heteroatoms activation at C(2) is competitive with activation at C(7) but in all cases coordination of the pyridinyl nitrogen is favored over oxygen, pyrrole nitrogen atoms and in particular sulfur [1-7].

The reactivity of sulfur containing aromatic heterocycles toward transition metal centers has been an active area of research due to the relevance of the complexes obtained towards understanding catalytic hydrodesulfurization (HDS) processes [8, 9]. The reactions of thiophene and derivatives with cluster complexes of the iron subgroup have also received considerable attention and it has been shown that the reactions of thiophenes with $[Fe_3(CO)_{12}]$ and $[Ru_3(CO)_{12}]$ lead to ring opening and ultimately to desulfurization of thiophenes [10]. Benzothiophene and dibenzothiophene correspond more closely to the major sulfur components in fossil fuels than thiophene itself [11]. The desulfurization of benzothiophene by S/Ru exchange in the reaction

between $[Ru_3(CO)_{12}]$ and benzothiophene has been reported by Deeming and co-workers [10d]. Recently, García et al. reported that $[Ru_3(CO)_{12}]$ reacts with dibenzothiophene to give the dinuclear complex $[Ru_2(C_{12}H_8)(CO)_6(\mu\text{-}CO)_6]$ by a double C-S bond activation-desulfurization process [12]. Both C-H and C-S bond activated products of thiophene, tetrahydrothiophene, benzothiophene and dibenzothiophene were obtained from their reactions with activated and/or unsaturated triosmium clusters [13-16]. However, the chemistry of S-heterocycles containing fused benzene rings is distinctly less developed than that of the corresponding N-heterocycles. Particularly, very little has been investigated on the synthesis of the electron-deficient complexes derived from S-heterocycles, although it might be expected that in the absence of a pyridinyl nitrogen that the S atom would coordinate and provide complexes similar to the N-benzoheterocyclic compounds $[Os_3(CO)_9\{\mu_3\text{-}\eta^2\text{-}(L\text{-}H)\}(\mu\text{-}H)]$. Very recently, we have reported that $[Ru_3(CO)_{12}]$ reacts with thianthrene in refluxing toluene to afford a mixture of novel tetra-,penta- and hexaruthenium clusters $[Ru_4(CO)_9(\mu\text{-}CO)_2(\mu_4\text{-}\eta^2\text{-}C_6H_4)(\mu_4\text{-}S)]$, $[Ru_5(CO)_{11}(\mu\text{-}CO)_2(\mu\text{-}\eta^3\text{-}C_{12}H_8S)(\mu_4\text{-}\eta^2\text{-}C_6H_4)(\mu_5\text{-}S)$ and $[Ru_6(CO)_{15}(\mu\text{-}CO)_2(\mu\text{-}\eta^3\text{-}C_{12}H_8S)(\mu_5\text{-}S)]$, respectively which were separated by chromatography and fully characterized [17] (Scheme 1). As part of an ongoing examination into the behavior of polydentate S heterocycles toward metal carbonyl clusters, we set out to investigate the reactivity of the labile osmium cluster $[Os_3(CO)_{10}(CH_3CN)_2]$ with thianthrene with the idea of synthesizing electron-deficient triosmium compounds bearing S-coordinated heterocycles analogous to the N-coordinated heterocyclic triosmium compounds $[Os_3(CO)_9\{\mu_3\text{-}\eta^2\text{-}(L\text{-}H)\}(\mu\text{-}H)]$.

Scheme 1 here

EXPERIMENTAL SECTION

General Comments

All reactions were performed under a nitrogen atmosphere using standard Schlenk techniques. Solvents were dried and distilled prior to use by standard methods. Thianthrene was purchased from Aldrich Chemical Company, Inc. and used as received. The starting compound $[Os_3(CO)_{10}(MeCN)_2]$ was prepared according to the literature method [18]. Infrared spectra were recorded on a Shimadzu FTIR 8101 spectrophotometer. ^1H and $^{31}P\{H\}$ NMR spectra were recorded on a Bruker DPX 400 spectrometer. Mass spectra were recorded on a Fisons Platform II ESI mass

spectrometer, with MeOH as mobile phase and NaOMe added as an ionization aid [19]. The m/z values reported are the strongest in the isotope envelope, and formulations were confirmed by matching isotope patterns with simulated ones generated with ISOTOPE [20]. Fast atom bombardment mass spectra were obtained on a JEOL SX-102 spectrometer using 3-nitrobenzyl alcohol as matrix and CsI as calibrant.

Reaction of $Os_3(CO)_{10}(MeCN)_2$ with thianthrene

A benzene solution (150 mL) of $[Os_3(CO)_{10}(MeCN)_2]$ (180 mg, 0.19 mmol) and thianthrene (82 mg, 0.38 mmol) was refluxed for 8 h. The solvent was removed under reduced pressure and the residue chromatographed by TLC on silica gel. Elution with hexane/CH_2Cl_2 (8:2 v/v) gave two bands. The first band afforded $[Os_3(CO)_9(\mu_3\text{-}\eta^2\text{-}C_{12}H_6S_2)(\mu\text{-}H)_2]$ (**1**) (30 mg, 15%) as yellow crystals after recrystallization from hexane/CH_2Cl_2 at – 4 ˚C (Anal. Calcd. for $C_{21}H_8O_9Os_3S_2$: C, 24.27; H, 0.78. Found: C, 24.38; H, 0.99%). IR (ν(CO), cyclohexane): 2107 s, 2080 ms, 2055 ms, 2035 ms, 2022 s, 2009 ms, 2000 s, 1986 s, 1955 m cm^{-1}. ^1H NMR ($CDCl_3$): δ 7.70 (d, J = 8.2 Hz, 1H), 7.45 (m, 2H), 7.23 (m, 2H), 6.84 (d, J = 8.2 Hz, 1H), –18.69 (s, 2H). MS (FAB): *m/z* 1040 (M^+), ESI-MS: *m/z* 1071 $[M+OMe]^-$. The second band gave $[Os_3(CO)_9(\mu_3\text{-}\eta^2\text{-}C_{12}H_7S_2)(\mu\text{-}H)]$ (**2**) (24 mg, 12%) as green crystals after recrystallization from hexane/CH_2Cl_2 at – 4 ˚C (Anal. Calcd. for $C_{21}H_8O_9Os_3S_2$: C, 24.27; H, 0.78. Found: C, 24.38; H, 0.93. IR (νCO, CH_2Cl_2): 2084 s, 2058 vs, 2027 vs, 1999 vs, 1964 m, 1950 m cm^{-1}. ^1H NMR ($CDCl_3$): δ 8.51 (d, J = 6.6 Hz, 1H), 8.36 (d, J = 7.3 Hz, 1H), 7.86 (d, J = 7.1 Hz, 1H), 7.61 (t, J = 7.1 Hz, 1H), 7.50 (d, J = 7.1 Hz, 1H), 7.36 (t, J = 7.3 Hz, 1H), 6.94 (t, J = 7.3 Hz, 1H), –12.08 (s, 1H). MS (FAB): *m/z* 1040 (M^+), ESI-MS: *m/z* 1071 [M+OMe].

Reaction of 2 with CO

Carbon monoxide gas was bubbled slowly through a $CDCl_3$ solution (0.75 mL) of **2** (10 mg, 0.010 mmol) in an NMR tube for 4 min. Immediate color changed from green to yellow was observed. The ^1H NMR indicated about 90% conversion to a new compound. The solvent was removed under reduced pressure and TLC separation of the residue as above gave two bands. The faster moving band afforded $[Os_3(CO)_{10}(\mu\text{-}\eta^2\text{-}C_{12}H_7S_2)(\mu\text{-}H)]$ (**3**) (6 mg, 60%) as yellow crystals after recrystallization from hexane/CH_2Cl_2 at – 4˚C (Anal. Calcd. for $C_{22}H_8O_{10}Os_3S_2$: C, 24.76; H, 0.76. Found: C, 24.92; H, 0.78). IR (νCO, CH_2Cl_2): 2082 m, 2054 vs, 2021 s, 1990 s, 1954 w, 1943

w cm^{-1}. ^1H NMR ($CDCl_3$): δ 7.23 (m, 3H), 7.47 (m, 4H), –14.30 (s, 1H). MS (FAB): m/z 1068 (M^+). The slower moving band gave a traces of **2**.

Reaction of 2 with PPh_3

Addition of solid PPh_3 (6 mg, 0.02 mmol) to a green CH_2Cl_2 solution (10 mL) of compound **2** (10 mg, 0.01 mmol) immediately changed the color to yellow and the solution was stirred for 30 min at room temperature. The solvent was evaporated to dryness and the residue chromatographed as above to give $[Os_3(CO)_9(PPh_3)(\mu\text{-}\eta^2\text{-}C_{12}H_7S_2)(\mu\text{-}H)]$ (**4**) (5 mg, 40%) as yellow crystals after recrystallization from hexane/CH_2Cl_2 at –4˚C. Anal. Calcd. for $C_{39}H_{23}O_9Os_3P_1S_2$: C, 35.99; H, 1.78. Found: C, 36.19; H, 1.85. IR (*ν*CO, hexane): 2089 w, 2046 s, 2024 s, 2012 s, 1990 m, 1975 w, 1967 w, 1962 w cm^{-1}. ^1H NMR ($CDCl_3$): δ 7.56 (m, 4H), 7.42 (m, 15H), 7.16 (m, 1H), 7.08 (m, 2H), –16.21 (d, $J_{P\text{-}H}$ = 12.8 Hz, 1H). $^{31}P\{^1H\}$ NMR ($CDCl_3$): δ –3.11 (s). MS (FAB): *m/z* 1302 (M^+). The slower moving band afforded the known compound $[Os_3(CO)_{10}(PPh_3)_2]$ (**5**) (3 mg, 23%) as orange crystals after recrystallization from hexane/CH_2Cl_2 at – 4˚C.

X-ray Crystallography

Single crystals of **2** suitable for X-ray diffraction were grown by slow diffusion of hexane into a dichloromethane solution at – 4 ˚C. X-ray intensity data for **2** were collected on a Bruker SMART with Mo-Kα X-rays using standard procedures and software. Semi-empirical absorption corrections were applied (SADABS) [21]. Structures were solved by direct methods and developed and refined on F^2 using the SHELX programmes [22] operating under WinGX [23]. The bridging hydride ligand was located from a difference map and refined. All other hydrogen atoms were included in calculated positions.

Electrochemistry

Electrochemical measurements were performed using a BAS CV-50W analyzer equipped with a standard three-electrode cell. The cell was designed to allow the tip of the reference electrode to approach closely to the working electrode. Voltammetric experiments were performed using aqueous Ag/AgCl as a reference electrode, a glassy carbon as a working electrode and platinum wire as the auxiliary electrode. Potential data are referenced to the ferreocene(0/+) couple, which is oxidized in CH_2Cl_2 at +0.48 V vs Ag/AgCl. Typically, a solution containing 1mM of the cluster

and 0.1 M supporting electrode (tetrabutylammonium hexafluorophosphate, Bu_4NPF_6) was prepared using freshly distilled dichloromethane. The solution was degassed prior to introducing the sample and also between runs. Positive feedback *i*R compensation was routinely applied.

Computational Details.

All calculations were performed using the Gaussian 03 package [24]. Geometry optimization of the cluster was performed at the B3PW91/LANLD2Z level for heavy atoms and at the B3PW91/6-31G** [17] for the light atoms. The nature of the stationary points was confirmed by normal mode analysis. No negative frequencies were found for the optimized geometry.

RESULTS AND DISCUSSION

Thermal treatment of the lightly stabilized bis-acetonitrile cluster $[Os_3(CO)_{10}(MeCN)_2]$ with thianthrene in refluxing benzene for 8 h resulted in the isolation of two new clusters $[Os_3(CO)_9(\mu_3\text{-}\eta^2\text{-}C_{12}H_6S_2)(\mu\text{-}H)_2]$ (**1**) and $[Os_3(CO)_9(\mu_3\text{-}\eta^2\text{-}C_{12}H_7S_2)(\mu\text{-}H)]$ (**2**) in 15% and 12% yields, respectively (Scheme 2). We were unable to obtain X-ray quality crystals of **1**, therefore the characterization is based on elemental analysis, infrared, ^{1}H NMR, ^{31}P-{^{1}H} NMR and mass spectral data. Compound **2** has been characterized by a combination of spectroscopic data and a single crystal X-ray diffraction analysis.

Scheme 2 here

The pattern of the IR spectrum of **1** in the carbonyl stretching region is very similar to that of $[Os_3(CO)_9(\mu_3\text{-}\eta^2\text{-}C_{12}H_6S)(\mu\text{-}H)_2]$, which was obtained from the reaction of $[Os_3(CO)_{10}(MeCN)_2]$ with dibenzothiaphene and characterized by X-ray diffraction, indicating that they are isostructural [15]. The FAB mass spectrum of **1** shows a molecular ion peak at m/z 1040 consistent with its formulation and fragmentation peaks due to the sequential loss of nine CO groups were also observed. No evidence for the formation of the decacarbonyl compound $[Os_3(CO)_{10}(\mu\text{-}\eta^2\text{-}C_{12}H_6S_2)(\mu\text{-}H)]$ has been obtained which should be the most probable intermediate to account for the formation of **1**. The decacarbonyl compound $[Os_3(CO)_{10}(\mu\text{-}\eta^2\text{-}C_8H_5S)(\mu\text{-}H)]$ was isolated and spectroscopically characterized in case of benzothiophene and subsequently converted into the nonacarbonyl dihydride compound $[Os_3(CO)_9(\mu_3\text{-}\eta^2\text{-}C_8H_4S)(\mu\text{-}H)_2]$ [15]. The aromatic region of the ^{1}H NMR spectrum of **1** contains two doublets at δ 7.70 and 6.84 (J = 8.2 Hz) and two multiplets

at δ 7.45 and 7.23 with the relative intensities 1:1:2:2, clearly indicating the activation of two C-H bonds of the thianthrene ligand. The hydride region of the spectrum shows a singlet hydride resonance of intensity 2 at δ –18.69. This is a typical chemical shift compared to those of similar dihydrido bridged nonacarbonyl triosmium complexes like $[Os_3(CO)_9(\mu_3\text{-}\eta^2\text{-}C_{12}H_6S)(\mu\text{-}H)_2]$ (δ –18.6.) [15] and $[Os_3(CO)_9(\mu_3\text{-}\eta^2\text{-}C_8H_4S)(\mu\text{-}H)_2]$ (δ –18.95) [13,15] for the two bridging hydride ligands. The hydride ligands are apparently dynamically averaged in the NMR spectrum at room temperature in all of these complexes as has been shown to be the case for the nonequivalent hydride ligands in the related $[Os_3(CO)_9(\mu_3\text{-SCCCHCH-})(\mu\text{-}H)_2]$ [25]. Compound **1** contains a triply bridging dehydrogenated thianthrene ligand bonded in a $\mu_3\text{-}\eta^2$-fashion to the cluster in a benzyne type manner [26] as has been found for complexes derived from benzothiophene and dibenzothiophene [13, 15]

The solid-state molecular structure of **2** is shown in Figure 1, crystal data are given in Table 1, and selected bond distances and bond angles are listed in Table 2. The structure consists of an isosceles triangle of osmium atoms with almost two equal metal-metal edges{Os(1)-Os(3) = 2.7977(2) and Os(2)-Os(3) = 2.8042(2) Å} and one significantly shorter metal-metal edge {Os(1)-Os(2) = 2.7574(2) Å}; all three metal-metal distances are significantly shorter than the average Os-Os distance of 2.875(3) Å found in $[Os_3(CO)_{12}]$ [27]. An intriguing structural feature of **2** is the coordination of the thianthrene ring to the cluster via the sulfur lone pair and a three-center-two-electron bond with C(10) which bridges the same edge of the triangle as the μ-hydride. Nine carbonyl groups, three bonded to each Os atom, complete the ligand shell of the cluster. The thianthrene ligand spans all three osmium atoms so as to cap one face of the Os_3 core. The metallated phenyl ring forms a slightly asymmetric bridge across the Os(1)-Os(2) edge {Os(1)-C(41) = 2.311(5) and Os(2)-C(41) = 2.277(4) Å}. This is distinctly different from the related benzoheterocycle nitrogen analogs where the Os-C bonds are perfectly symmetrical within experimental precision [1-7]. The hydride ligand was crystallographically located (refined) across the Os(1)- Os(2) edge of the triangle, sitting *trans* to carbonyl groups CO(13) and CO(23) and bent down towards the opposite face of the triangle occupied by the $\mu_3\text{-}\eta^2\text{-}C_{12}H_7S_2$ ligand. This overall trend in relative bond lengths is similar to those observed in the quinoline compound $[Os_3(CO)_9\{\mu_3\text{-}\eta^2\text{-}C_9H_5(4\text{-}CH_3)N\}(\mu\text{-}H)]$ [1a] and the quinoxaline compound $[Os_3(CO)_9(\mu_3\text{-}\eta^2\text{-}C_8H_5N_2)(\mu\text{-}H)]$ [1c]. The thianthrene ligand is slightly less folded about the S…S vector in the complex (dihedral angle 134^o) than in the free ligand (dihedral angle 127^o). The ring of the ligand

attached to the Os_3 triangle effectively bisects the cluster in an orientation that is almost perpendicular (dihedral angle 84.9°) to the metal plane [28]. The Os-S bond distance of Os(3)-S(1) = 2.426(1) Å is similar to the Os-S bond distance in $[Os_3(CO)_{10}(\mu\text{-}SCCHC_6H_5\text{-})(\mu\text{-}Br)]$ {2.411(5) Å}[13] and $[Os_3(CO)_9(PPh_3)(\mu\text{-}SCHCH_2CH_2CH_2\text{-})(\mu\text{-}H)]$ {2.407(1) Å} [29]. The average S-C distance of 1.769(5) Å is typical of a carbon-sulfur single bond, however, the S-C distances involving the coordinated sulfur atom {S(1)-C(42) = 1.784(4) and S(1)-C(51) = 1.790(4) Å}are longer than those involving an uncoordinated sulfur atom{S(2)-C(43) = 1.769(5) and S(2)-C(52) = 1.769(5) Å}as a result of the effect of coordination to the metal core. The average C-C bond distances in the two benzenoid rings are normal {1.394(6) Å}. The aromatic nature of the rings remains relatively unperturbed, making **2** a unique example of an electron-deficient trimetallic species containing a μ_3-heterocyclic (sulfur containing) aromatic capping ligand. The valence electron count for **2** is 46, which is 2 less than expected 48-electron count for closed trimetallic clusters.

Figure 1 here

Tables 1and 2 here

The spectroscopic data of **2** are fully consistent with the solid-state structure. The pattern of the infrared spectrum of **2** in the carbonyl region is very similar to those of the electron-deficient 4-methylquinoline $[Os_3(CO)_9\{\mu_3\text{-}\eta^2\text{-}C_9H_5(4\text{-}CH_3)N\}(\mu\text{-}H)]$, and quinoxaline, $[Os_3(CO)_9(\mu_3\text{-}\eta^2\text{-}C_8H_5N_2)(\mu\text{-}H)]$ clusters which have been characterized by X-ray diffraction studies [4]. The aromatic region of the ^{1}H NMR spectrum contains seven well-separated equal intensity signals, four doublets at δ 8.51, 8.36, 7.86 and 7.50 and three apparent double doublets at δ 7.61, 7.36 and 6.94, each integrating for one hydrogen. The hydride region of the spectrum contains a singlet at δ –12.08 due to the bridging hydride ligand. The ESI mass spectrum contain the appropriate $[M+OMe]^-$ peak for the molecular mass of 1040 Daltons.

The electron-deficiency in **2** is demonstrated by its facile and reversible addition reaction with CO. Thus by bubbling CO (1 atm) through a toluene solution of **2** for 4 min, about 90% conversion into yellow $[Os_3(CO)_{10}(\mu_2\text{-}\eta^2\text{-}C_{12}H_7S_2)\ (\mu\text{-}H)]$ (**3**) is achieved as evidenced by ^{1}H NMR Scheme 2). Compound **3** was isolated in 60% yield after chromatographic separation alone with traces of unconsumed **2**. Conversion of **3** back to **2** is achieved at 80 °C in refuxing benzene. Compound **3** was characterized by elemental analysis, infrared and ^{1}H NMR and mass spectral data. The pattern of the infrared spectrum clearly indicates a 4:3:3 carbonyl distribution similar to

the related decacarbonyl nitrogen benzoheterocycle complexes [1-7]. The mass spectrum shows the molecular ion peak at m/z 1068 and ions due to the sequential loss of ten carbonyl groups. The ^{1}H NMR spectrum exhibits apart from two multiplets at δ 7.23 and 7.47 integrating for 3 and 4 protons, respectively in the aromatic region, a high field resonance at δ –14.30, assigned to the bridging hydride. By a comparison of the IR and ^{1}H NMR data with that of $[Os_3(CO)_{10}(\mu\text{-}\eta^2\text{-}C_9H_6N)(\mu\text{-}H)]$ which was characterized XRD studies [30], a probable structure for **3** is depicted in Scheme 2. It represents a 48-electron cluster with a three electron donor $\mu\text{-}\eta^2\text{-}C_{12}H_7S_2$ ligand bound through the sulfur and C(2) carbon atoms to the cluster framework.

Addition of two equivalents of PPh_3 to a green solution of compound **2** immediately turns to yellow which after chromatographic separation gave the adduct $[Os_3(CO)_9(PPh_3)(\mu_2\text{-}\eta^2\text{-}C_{12}H_7S_2)(\mu\text{-}H)]$ (**4**) and the substitution product $[Os_3(CO)_{10}(PPh_3)_2]$ (**5**). The spectroscopic data of **4** are consistent with the formulation. In agreement with the presence of a $\mu_2\text{-}\eta^2\text{-}C_{12}H_7S_2$ and a PPh_3 ligand in **4**, the ^{1}H NMR spectrum contains four multiplets at δ 7.56, 7.42, 7.16 and 7.08 with the relative intensities 4:15:1:2. The hydride region of the spectrum contains a doublet at δ –16.21 with a phosphorus-hydrogen coupling of 12.8 Hz. The $^{31}P\{^1H\}$ NMR exhibits a singlet at δ –3.11. The formulation of **4** is supported by its FAB mass spectrum, which confirms a mass of 1302 Daltons. By a comparison of the IR, ^{1}H NMR and $^{31}P\{^1H\}$ NMR data with those of $[Os_3(CO)_9(PPh_3)(\mu\text{-}\eta^2\text{-}C_9H_6N)(\mu\text{-}H)]$ which was obtained from the addition of PPh_3 to the electron-deficient of $[Os_3(CO)_9(PPh_3)(\mu_3\text{-}\eta^2\text{-}C_9H_6N)(\mu\text{-}H)]$ and characterized by x-ray crystallography, the depicted for **4** where the phosphine ligand is on the Os atom bound to the carbon atom of the heterocycle is most likely, as shown in Scheme 2 [1a]. The formation of **5** is probably the result of nucleophilic attack at the metal core followed by reduction elimination of thianthrene. The previously reported compound **5** was identified by comparison of its spectroscopic properties with the literature values [31]. This facile phosphine induced reductive elimination of the heterocyclic ligand has not been previously observed with the nitrogen analogs of **2** and points to a distinct difference in the bonding between the cluster and the ligand in this new complex (*vide infra*).

The previously reported electron deficient benzoheterocycle nitrogen triosmium clusters, $[Os_3(CO)_9\{\mu_3\text{-}\eta^2\text{-}(L\text{-}H)\}(\mu\text{-}H)]$ were all electrochemically active. In some cases (L = phenanthridine, 5,6-benzoquinoline, 4-quinoline carboxaldehyde) reversible reductions were observed and relatively stable carbanions were formed. Only irreversible oxidations were observed. In other instances (L=quinoline, quinoxaline, benzothiazole, benzoxazole and benzimidazole)

irreversible reductions and oxidation were observed [1b, 1g, 4]. In order to compare the electrochemical behavior of this class of electron deficient complexes with **2** we measured its redox potentials in CH_2Cl_2 and report them here relative to the Fc/Fc^+ couple. Compound **2** shows an irreversible reduction at -1.54 V and an irreversible oxidation at +0.574 V at a scan rate of 50 mV/s. These irreversible potentials are significantly different from those of quinoline which exhibits two irreversible reductions at -1.38 and -1.99 V and an irreversible oxidation at +0.14 V. It might be expected that the less electronegative sulfur heterocycle would show a more positive oxidation potential and a slightly more negative first reduction but it was a bit surprising that the presence of a third aromatic ring did not render the reduction reversible as is the case for the electron deficient clusters of tricyclic triosmium clusters of phenanthridine and 5,6-benzoquinoline. It would appear that the disposition of the third ring has an influence on the stability of the radical anion resulting from electrochemical reduction.

In order to better understand the electron acceptor properties of **2** and to compare its overall electronic structure with related clusters previously investigated by computational methods we undertook a Density Functional Theory study of this novel cluster. All calculations were performed using the Gaussian 03 package [24]. Geometry optimization of the cluster was performed at the B3PW91/LANLD2Z level for heavy atoms and at the B3PW91/6-31G** for the light atoms. The nature of the stationary points was confirmed by normal mode analysis. No negative frequencies were found for the optimized geometry. It can be seen from the data in Tables 2 and 3 that calculated bond distances and angles are in reasonable agreement with the experimental values. The computed metal-metal bonds and metal-ligand bonds are slightly elongated with respect to the experimental ones (~0.03-0.07 Å) and this has been previously noted for these types of complexes in the absence of applying an f polarization [32]. The overall pattern of the carbonyl stretching frequencies are qualitatively duplicated by the calculations but they are shifted by 100 cm^{-1} and curiously, one additional peak is observed experimentally which we tentatively assign to the hydride ligand (1950 cm^{-1}).

Table 3 here

Most interestingly, the HOMO in **2** is strictly metal based while the LUMO has mainly ligand contributions with some metal involvement at the unique osmium atom. In cases where reversible reduction and stable radical anions of this structural type are observed (e. g. phenanthridine, 5,6-benzoquinoline) involvement of the hydride-bridged edge of the cluster in the

LUMO is observed and significant spin density on the hydride is present based on both experimental and computational evidence [4a]. This interaction leads to a more delocalized radical anion with the associated stabilization [33]. This interaction is conspicuously missing in **2** and probably explains why this tricyclic aromatic triosmium cluster does not show reversible one-electron reductions. This segregation of metal and ligand participation in the constitution of the molecular orbitals of **2** carries over to the H-1 and H-2 orbitals (Figure 3) until finally at H-3 significant participation of both metal and ligand orbitals is seen (Figure 4). Again this is contrast with the results of previous DFT studies of related electron deficient clusters where participation of both metal core and ligand in the occupied and unoccupied molecular orbitals is pervasive [4, 33, 34]. The non-planarity of this heterocyclic system in both the solid state and computed structures surely makes a strong contribution to the orbital pictures presented in Figures 2-4 and may also be the route cause of the instability of the radical anion.

Figures 2-4 here

CONCLUSIONS

The present work reports an unprecedented example of an electron-deficient triosmium cluster bearing a sulfur coordinated heterocyclic ligand whose carbocyclic ring is also bound to the cluster via a three centre two electron bond. The synthesis of compound **2** has opened up the possibility of exploring the synthesis of this so-far-unknown class of compounds. The electron-deficiency in **2** has been demonstrated by its facile reactions with CO and PPh_3. Complex **2** however, is distinctly different electronically than the previously reported hetero-polycylic triosmium complexes in that there seems to be less direct electronic communication between the ligand and the metal core based on the electrochemical behavior, the DFT results and the facile displacement of the thianthrene ring from the cluster by phosphines. It will be interesting to see if the alteration of the reactivity of the aromatic ring observed with the former complexes will extend to sulfur based electron deficient complexes such as **2**.

SUPPLEMENTARY MATERIAL

Crystallographic data for the structural analyses have been deposited with the Cambridge Crystallographic Data Center, CCDC No. 650731 for compound **2.** Copies of this information may

be obtained free of charge from the Director, CCDC, 12 Union Road, Cambridge, CB2 1 EZ, UK (fax: +44-1223-336033; e-mail: deposit@ccdc.cam.ac.uk or www: http://www.ccdc.ac.uk)

ACKNOWLEDGEMENTS

We thank Dr. Tania Groutso, University of Auckland for collection of X-ray intensity data. One of us (AKR) gratefully acknowledges the University Grants Commission of Bangladesh for a Scholarship. Support for this research by the Department of Energy (E.R., grant # DE-FG02-01ER45869) is also gratefully acknowledged.

REFERENCES

1. (a) S. E. Kabir, D. S. Kolwaite, E. Rosenberg, K. I. Hardcastle, W. Cresswell, and J. Grindstaff (1995). *Organometallics* **14**, 3611. (b) E. Arcia, E. Rosenberg, D. S. Kolwaite, K. I. Hardcastle, J. Ciurash, R. Duque, R. Gobetto, L. Milone, D. Osella, M. Botta, W. Dastru', A. Viale, and I. Fiedler (1998). *Organometallics* **17**, 415. (c) M. J. Abedin, B. Bergman, R. Holmquist, R. Smith, E. Rosenberg, J. Ciurash, K. I. Hardcastle, J. Roe, V. Vazquez, C. Roe, S. E. Kabir, B. Roy, S. Alam, and K. A. Azam (1999). *Coord. Chem. Rev.* **190-192**, 175. (d) B. Bergman, R. Holmquist, R. Smith, E. Rosenberg, K. I. Hardcastle, M. Visi, and J. Ciurash (1998). *J. Am. Chem. Soc.* **120**, 12818. (e) R. Smith, E. Rosenberg, K. I. Hardcastle, V. Vazquez, and J. Roh (1999). *Organometallics* **18**, 3519. (f) A. V. Bar Din, B. Bergman, E. Rosenberg, R. Smith, W. Dastru', R. Gobetto, L. Milone, and A. Viale (1998). *Polyhedron* **17**, 2975. (g) E. Rosenberg, Md. J. Abedin, D. Rokhsana, D. Osella, L. Milone, N. Nervi, and I. Fiedler (2000). *Inorg. Chim. Acta* **300-302**, 769.
2. S. E. Kabir, K. M. A. Malik, H. S. Mandal, Md. A. Mottalib, Md. J. Abedin, and E. Rosenberg (2002). *Organometallics* **21**, 2593.
3. E. Rosenberg, S. E. Kabir, Md. J. Abedin, and K. I. Hardcastle (2004). *Organometallics* **23**, 3982.

4. (a) C. Nervi, R. Gobetto, L. Milone, A. Viale, E. Rosenberg, D. Rokhsana, and I. Fiedler (2003). *Chem. Eur. J.* **9**, 5749. (b) E. Rosenberg, D. Rokhsana, C. Nervi, R. Gobetto, L. Milone, A. Viale, I. Fiedler, and M. A. Botavina (2004). *Organometallics* **23**, 215. (c) E. Rosenberg, M. J. Abedin, D. Rokhsana, A. Viale, W. Dastru', R. Gobetto, L. Milone, and K. I. Hardcastle (2002). *Inorg. Chim. Acta* **334**, 343.
5. Md. A. Mottalib, N. Begum, S. M. T. Abedin, T. Akter, S. E. Kabir, Md. A. Miah, D. Rokhsana, E. Rosenberg, G. M. G. Hossain, and K. I. Hardcastle (2005). *Organometallics* **24**, 4747.
6. E. Rosenberg, F. Spada, K. Sugden, B. Martin, R. Gobetto, L. Milone, and A. Viale (2004). *J. Organomet. Chem.* **689**, 4729.
7. E. Rosenberg, F. Spada, K. Sugden, B. Martin, R. Gobetto, L. Milone, A. Viale,and J. Fiedler (2003). *J. Organomet. Chem.* **668**, 51.
8. (a) M. A. Reynolds, I. A. Guzei, and R. J. Angelici (2003). *Inorg. Chem.* **42**, 2191. (b) M. A. Reynolds, I. A. Guzei, and R. J. Angelici (2000). *J. Chem. Soc., Chem. Commun*. 513. (c) M. A. Reynolds, I. A. Guzei, and R. J. Angelici (2001). *Organometallics* **20**, 1071. (d) J. Chen, and R. J. Angelici (1999). *Organometallics* **18**, 5721. (e) R. J. Angelici (2005). In *Encyclopedia of Inorganic Chemistry, 2nd Ed.*; R. B. King (Ed.) Wiley: New York, Vol. 3, p 1860. (f) R. J. Angelici (2001). *Organometallics* **20**, 11259. (g) R. J. Angelici (1990). *Coord. Chem. Rev.* **105**, 61.
9. (a) R. C. A. Mills, and J. M. Boncella (2001). *Chem. Commun.* 1506. (b) T. B. Rauchfuss (2004). *Prog. Inorg. Chem.* **43**, 14. (m) K. E. Janak, J. M. Tanski, D. G. Churcill, and G. J. Perkin (2002). *J. Am. Chem. Soc.* **124**, 4182. (c) M. L. Spera, and W. D. Harman (1997). *J. Am. Chem. Soc.* **119**, 8843. (d) M. L. Spera, and W. D. Harman (1999). *Organometallics* **18**, 2988. (e) C. Bianchini, V. Herrera, M. Jimenez, A. Meli, R. A. Sanchez-Delgado, and F. Vizza (1995). *J. Am. Chem. Soc.* **117**, 8567.
10. (a) H. D. Kaesz, R. B. King, T. A. Manuel, L. D. Nichols, F. G. A. Stone (1960). *J. Am. Chem. Soc.* 82, 4749. (b) A. E. Ogilvy, M. Draganjac, T. B. Rauchfuss, and F. R. Wilson (1988). *Organometallics* **7**, 1171. (d) A. J. Arce, Y. De Sanctis, A. Karam, and A. J. Deeming (1994). *Angew. Chem., Int. Ed. Engl.* **33**, 1381. A. J. Arce, Y. De Sanctis, and A. J. Deeming (1986). *J. Organomet. Chem.* **311**, 371.

11. (a) H. Topsoe, and B. C. Gates (1977). *Polyhedron* **16**, 3212. (b) B. C. Gates, J. R. Katzer, and C. A. Schuit, Chemistry of Catalytic Processes; MacGraw Hill: New York, 1979; pp 1433-1443. (c) D. R. Kilanowski and B. C. Gates (1980). *J. Catal*. **62**, 70.

12. A. Chehata, A. Oviedo, A. Arévalo, S. Bernès, and J. Garcéa (2003). *Organometallics* **22**, 1585.

13. R. D. Adams, and X. Qu (1995). *Organometallics* **14**, 2238.

14. 13. R. D. Adams, M. P. Pompeo, W. Wu, and J. H. Yamamoto (1993). *J. Am. Chem. Soc*. **115**, 4207.

15. A. J. Arce, A. Karam, Y. De Sanctis, M. V. Capparelli, and A. J. Deeming (1999). *Inorg. Chim. Acta* **285**, 277.

16. S. E. Kabir, M. A. Miah, N. C. Sarkar, G. M. G. Hussain, K. I. Hardcastle, E. Nordlander, and E. Rosenberg (2005). *Organometallics* **24**, 3315.

17. M. R. Hassan, S. E. Kabir, B. K. Nicholson, E. Nordlander, and M. N. Uddin *Oganometallics* (in press).

18. J. Lewis, P. J. Dyson, B. J. Alexander, B. F. G. Johnson, C. M. Martin, J. M. G. Nairn, E. Parsini (1993). *J. Chem. Soc., Dalton Trans.* 519.

19. W. Henderson, J. S. McIndoe, B. K. Nicholson, and P. J. Dyson (1998). *J. Chem. Soc., Dalton Trans.,* 519.

20. L. J. Arnold (1992). *J. Chem. Educ*. **69**, 811.

21. R. H. Blessing (1995). *Acta Cryst*. **A51**, 33.

22. G. M. Sheldrick (1997). SHELX97 Programs for the solution and refinement of crystal structures, University of Göttingen, Germany.

23. L. J. Farrugia, WinGX, Version 1.70.01, University of Glasgow, UK; L. J. Farrugia (1999). *J. Appl. Cryst*., **32**, 837.

24. M. J. Frisch, G. W. Trucks, H. B. Schlegel, G. E. Scuseria, M. A. Robb, J. R. Cheeseman, J. A. Jr. Montgomery, T. Vreven, K. N. Kudin, J. C. Burant, J. M. Millam, S. S. Iyengar, J. Tomasi, V. Barone, B. Mennucci, B. Cossi, G. Scalmani, N. Rega, G. A. Petersson, H. Nakatsuji, M. Hada, M. Ehara, K. Toyota, R. Fukuda, J. Hasegawa, M. Ishida, T. Nakajima, Y. Honda, O. Kitao, H. Nakai, M. Klene, X. Li, J. E. Knox, H. P. Hratchian, J. B. Cross, C. Adamo, J. Jaramillo, R. Gomperts, R. E. Stratmann, O. Yazyev, A. J. Austin, R. Cammi, C. Pomelli, J. Ochterski, P. Y. Ayala, K. Morokuma, G. A. Voth, P. Salvador, J. J. Dannenberg, V. G. Zakrzewski, S. Dapprich, A. D. Daniels, M. C. Strain, O. Farkas, D. K. Malick, A. D. Rabuck, K. Raghavachari, J. B. Forestman, J.

V. Ortiz, Q. Cui, A. G. Baboul, S. Clifford, J. Cioslowski, B. B. Stefanov, G. Liu, A. Liashenko, P. Piskorz, I. Komaromi, R. L. Martin, D. J. Fox, T. Keith, M. A. Al-Laham, C. Y. Peng, A. Nanayakkara, M. Challacombe, P. M. W. Gill, B. Johnson, W. Chen, M. W. Wong, C. Gonzales, and J. A. Pople (2004). Gaussian 03. (revision C.02). Wallingford CT, Gaussian Inc.

25. A. J. Deeming, A. J. Arce, Y. De Sanctis, M. W. Day, and K. I. Hardcastle(1989). *Organometallics* **8**, 1408.

26. R. J. Goudsmit, B. F. G. Johnson, J. Lewis, P. R. Raithby, and M. J. Rosales (1983). *J. Chem. Soc., Dalton Trans.* 2257.

27. M. R. Churchill, and B. G. DeBoer (1977). *Inorg. Chem*. 16, 878.

28. S. B. Larson, G. E. Martin, S. H. Simonsen, K. Smith, and S. Puig-Torres (1984): *Acta Cryst*. **C40**, 103.

29. G. N. Glavee, L. M. Daniels and R. J. Angelici (1989). *Organometallics*, **8**, 1856.

30. J. Akter, G. M. G. Hossain, S. E. Kabir, and K. M. A. Malik (2002). *J. Chem. Crystallogr*. **30**, 381.

31. W. K. Leong, and Y. Liu (1999) *J. Organomet. Chem*. **584**, 174.

32. D. G. Musaev, T. Nowroozi-Isfahani, K. Morokuma, E. Roseneberg (2005) *Organometallics* **24** 5973.

33. D. G. Musaev, T.Nowroozi-Isfahani, K. Morokuma J. Abedin, E. Rosenberg K. I. Hardcastle (2006) *Organometallics* **25**, 203.

34. T. Nowroozi-Isfahani, D. G. Musaev, K. Morokuma, E. Rosenberg (2006) *Inorg. Chem.* **45**, 4963.

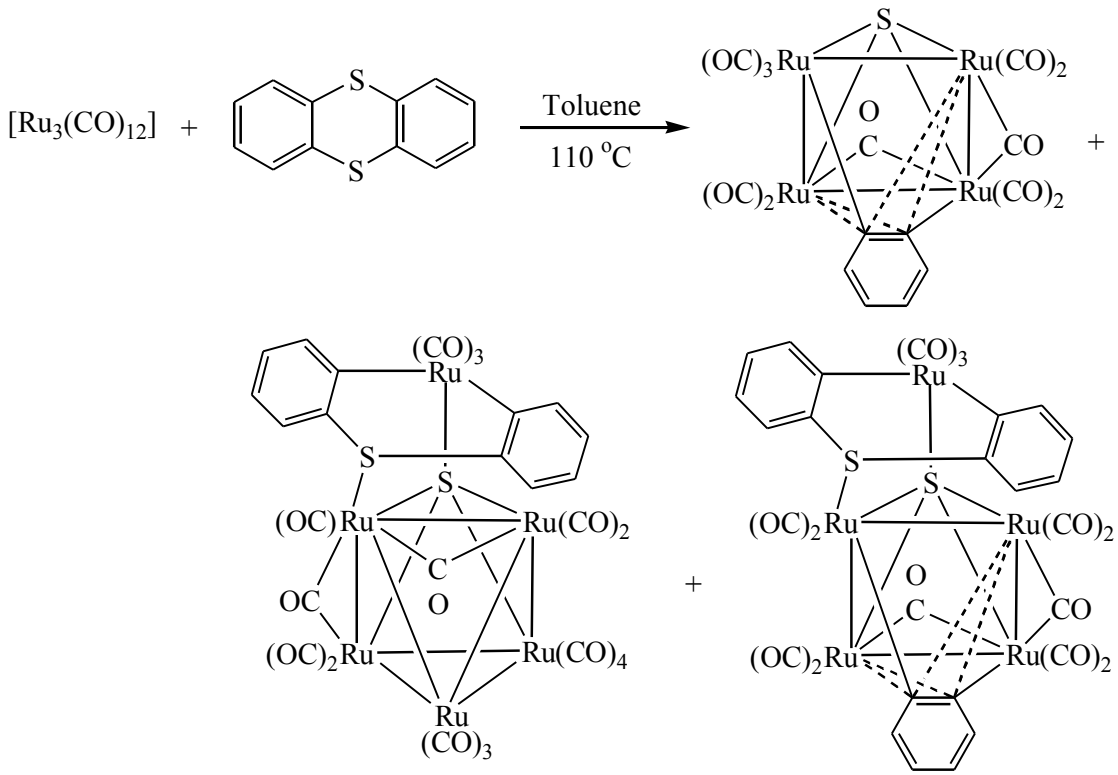

Scheme 1

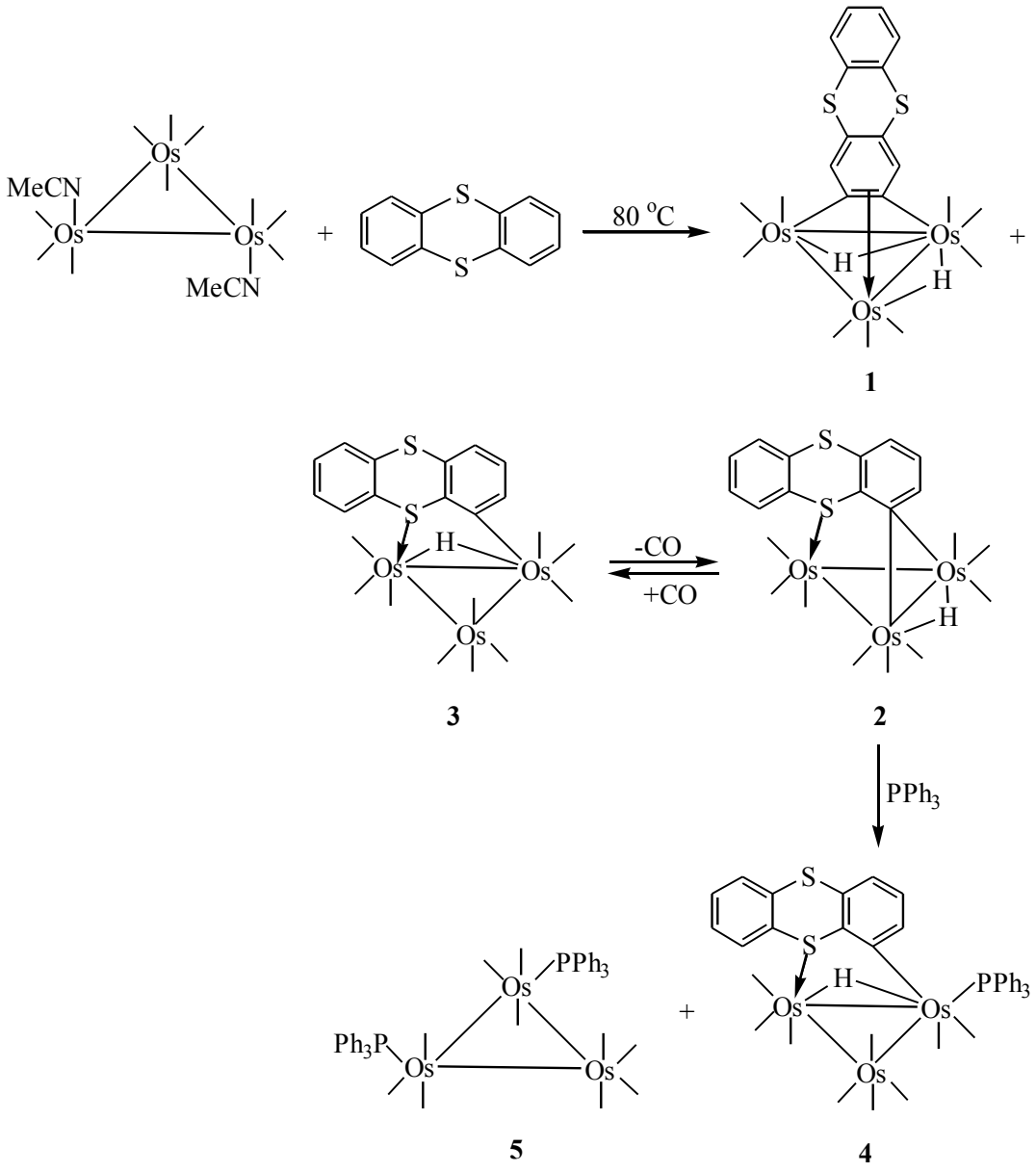
MeCN
Os
Os
Os
MeCN
+
S
S
80 °C
S
S
Os
Os
H
H
Os
+
1
S
S
H
Os
Os
Os
3
-CO
+CO
S
S
Os
Os
H
Os
2
PPh3
S
S
H
Ph3P
PPh3
Os
Os
Os
Os
Os
+
5
4

Scheme 2

Table 1.

Crystallographic Data and Structure Refinement for $[Os_3(CO)_9(\mu_3\text{-}\eta^2\text{-}C_{12}H_7S_2)(\mu\text{-}H)]$ (**2**)

	2
Empirical formula	$C_{21}H_8O_9Os_3S_2$
Formula weight	1038.99
Crystal system	Monoclinic
Space group	*P*2(1)/*n*
Temperature	89(2) K
Wavelength	0.71073 Å
a (Å)	10.5666(1)
b (Å)	13.8486(2)
c (°)	16.5331(2)
α (°)	90
β (°)	100.95(1)
γ (°)	90
Volume, Å^3	2375.28(5)
Z	4
D_{calc}, (Mg/m^3)	2.905
μ (Mo Kα), mm^{-1}	16.234
F(000)	1864
Crystal size, mm^3	0.28 x 0.26 x 0.20
θ range, deg	1.93 to 26.37
Index ranges	$-12 \le h \le 13$ $-9 \le k \le 7$ $-19 \le l \le 20$
Reflections collected	13998
Independent reflections	4847 [*R*(int) = 0.0211]
Max. and min. transmn	0.0850 and 0.0497
Refinement method	Full-matrix least-squares on F^2
Data/restraints/parameters	4847 / 0 / 320
Goodness-of-fit on F^2	1.020
Final *R* indices [$I>2\sigma(I)$]	R_1 = 0.0183 wR_2 = 0.0388
R indices (all data)	R_1 = 0.0208 wR_2 = 0.0398
Largest diff peak and hole, e.Å^{-3}	0.740 and -0.839

Table 2
Selected Bond Distances (Å) and Angles (°) for $[Os_3(CO)_9(\mu_3\text{-}\eta^2\text{-}C_{12}H_7S_2)(\mu\text{-}H)]$ (**2**)

Os(1)-Os(2)	2.7574(2)	C(42)-C(43)	1.404(6)
Os(1)-Os(3)	2.7977(2)	C(43)-C(44)	1.384(6)
Os(2)-Os(3)	2.8042(2)	C(44)-C(45)	1.391(7)
Os(2)-H(1)	1.77(5)	C(45)-C(46)	1.376(7)
Os(1)-H(1)	1.71(5)	C(51)-C(56)	1.391(6)
Os(1)-C(41)	2.311(5)	C(51)-C(52)	1.402(6)
Os(2)-C(41)	2.277(4)	C(52)-C(53)	1.391(6)
Os(3)-S(1)	2.4261(11)	C(53)-C(54)	1.375(7)
C(41)-C(46)	1.423(6)	C(54)-C(55)	1.390(7)
C(41)-C(42)	1.424(6)	C(55)-C(56)	1.380(7)
S(1)-C(42)	1.784(4)	S(1)-C(51)	1.790(4)
S(2)-C(52)	1.763(5)	S(2)-C(43)	1.916(5)
C(41)-Os(1)-Os(2)	52.51(11)	C(41)-Os(2)-Os(1)	53.62(11)
C(41)-Os(1)-Os(3)	82.91(11)	C(41)-Os(2)-Os(3)	83.35(11)
Os(2)-Os(1)-Os(3)	60.630(6)	C(41)-Os(2)-H(1)	82.1(17)
C(41)-Os(1)-H(1)	82.2(18)	S(1)-Os(3)-Os(1)	88.24(3)
Os(2)-Os(1)-H(1)	38.4(18)	S(1)-Os(3)-Os(2)	82.94(3)
Os(3)-Os(1)-H(1)	84.1(18)	C(52)-S(2)-C(43)	101.6(2)
Os(2)-C(41)-Os(1)	73.88(14)	Os(1)-Os(2)-Os(3)	60.396(6)
Os(2)-Os(1)-C(12)	111.23(14)	Os(1)-Os(3)-Os(2)	58.974(6)
Os(2)-Os(1)-C(11)	121.11(14)	Os(1)-Os(2)-C(21)	121.46(14)
C(42)-S(1)-C(51)	101.9(2)	Os(1)-Os(2)-C(22)	110.52(14)

Table 3

Computational Data for Complex 2

Selected Computed Distances (Å)	
Os1-Os2	2.79077
Os2-Os3	2.82457
Os1-Os3	2.82104
Os2-H1	1.83331
Os3-H2	1.83739
Os3-S1	2.53996
S1-C51	1.84735
S1-C42	1.83274
S2-C43	1.82225
S2-C52	1.82023
Os1-C41	2.34220
Os2-C41	2.29571

Computed Angles (degrees)	
Os1-Os2-Os3	60.31169
Os2-Os1-Os3	60.43779
Os2-Os3-Os1	59.25052
Os1-H1-Os2	98.97838
C51-S1-C42	101.72466
C52-S2-C43	100.30834
Os1-C41-Os2	73.98013

Computed CO frequencies	
ν (cm^{-1})	relative intensity
2086	725
2103	1267
2121	1256
2151	1670
2173	563

Relative orbital energy (eV)	
L+4	- 0.051
L+3	- 0.052
L+2	- 0.057
L+1	- 0.069
LUMO	- 0.111
HOMO	- 0.220
H-1	- 0.245
H-2	- 0.252
H-3	- 0.270
H-4	- 0.271

Captions to Figures

Fig. 1: Solid-state molecular structure of $[Os_3(CO)_9(\mu_3\text{-}\eta^2\text{-}C_{12}H_7S_2)(\mu\text{-}H)]$ (**2**). Thermal ellipsoids are drawn at 35% probability level.

Fig. 2: (A) HOMO, orbital of **1**. (B) LUMO, orbital of **1**. $\Delta En_{(HOMO\text{-}LUMO)} = 0.109$ eV = 879 cm^{-1}.

Fig. 3: H-1 (left) and H-2 (right) bonding orbitals of **2**.

Fig. 4: H-3 bonding orbital of **2**

Figure 1

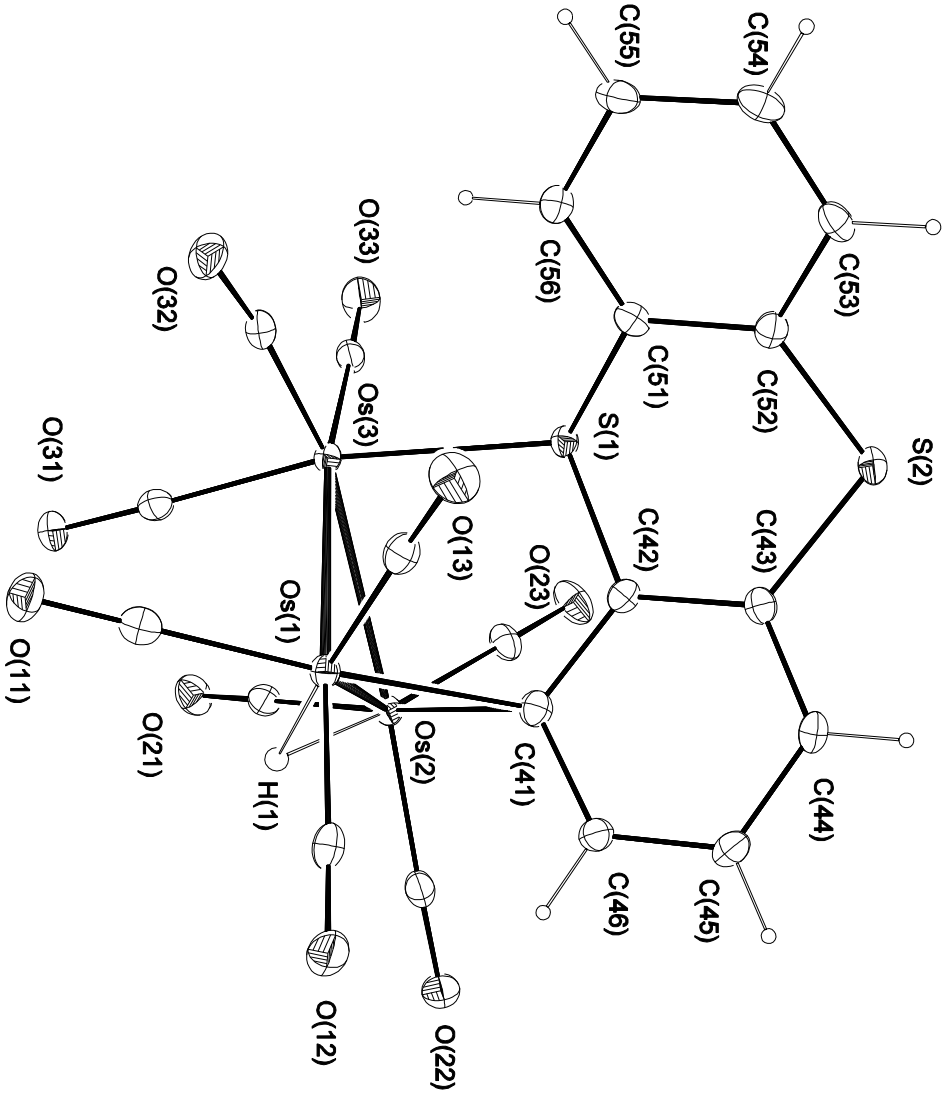
C(55)
C(54)
C(56)
C(53)
O(33)
O(32)
C(51)
C(52)
Os(3)
S(1)
S(2)
O(31)
O(13)
C(42)
C(43)
O(23)
Os(1)
O(11)
O(21)
Os(2)
C(41)
C(44)
H(1)
C(46)
C(45)
O(12)
O(22)

Figure 2

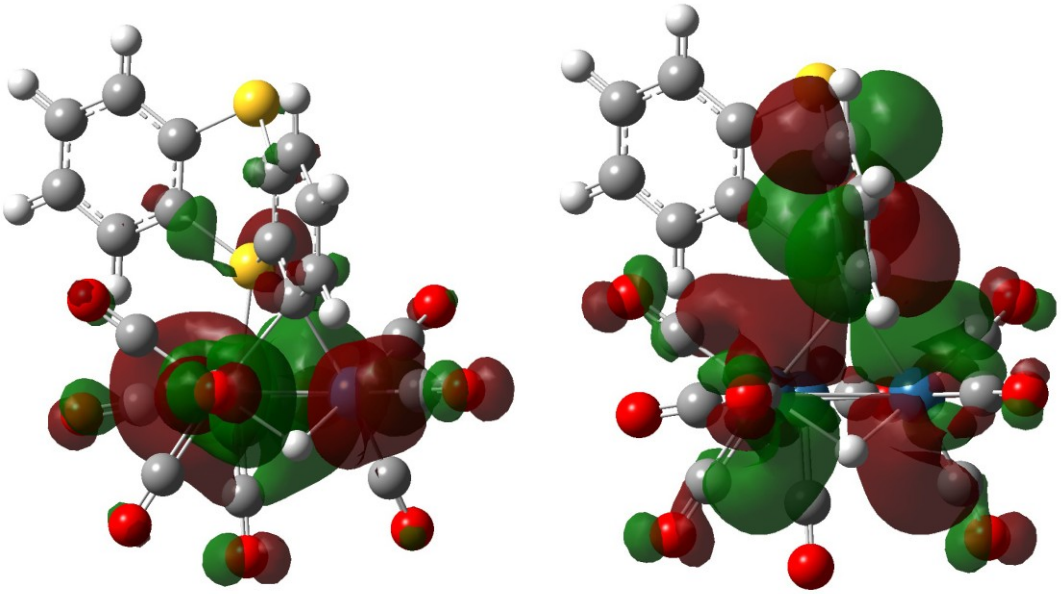

Figure 3

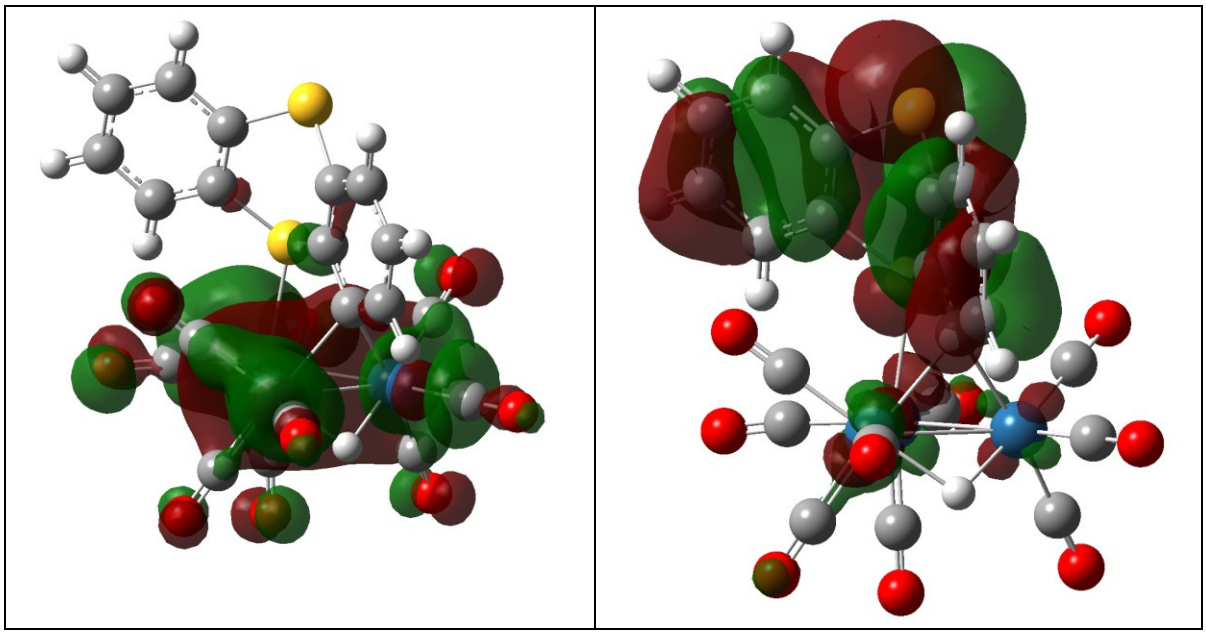

Figure 4